THE JOURNAL OF PROSTHETIC DENTISTRY

RESEARCH AND EDUCATION

Evaluation of the biomechanics of Aramany class I obturators of different designs using numerical and experimental methods. Part II: Stress distribution

Mohammed A. Mousa, BDSc, MDSc, MFDs, PhD,[a]
Adam Husein, BDS, GradDipClinDent, DClinDent (Prosthodontics),[b] Mohamed I. El-Anwar, BSc, MSc, PhD,[c]
Azirrawani Ariffin, BDS, MClinDent, MPROS,[d] and
Johari Yap Abdullah, B.S. & I.T., GradDip ICT, MSc, PhD (Craniofacial Biology)[e]

ABSTRACT

Statement of problem. Evidence regarding stress evaluations of removable obturators with Aramany class I defects is lacking. Whether the stress distribution on Aramany class I prostheses can be improved by modifying the currently used designs is also unclear.

Purpose. The purpose of part II of this study was to evaluate the stress distribution in different designs of Aramany class I obturators using finite element analysis (FEA) and photoelastic stress analysis.

Material and methods. Four finite element and 8 photoelastic models, including 2 acrylic resin base obturators retained with 2 Adams clasps, 2 linear, 2 tripodal, and 2 fully tripodal design obturators, were used in this study. The frameworks were fabricated on the casts obtained from a modified printed model. Vertical and oblique loads were applied on 2 points (anterior and posterior) of the models. The quantitative measurement was done by measuring the fringe orders and von Mises values to compare the influences of occlusal forces on the obturator components and their supporting structures. The qualitative evaluation was done by visual color mapping to identify the stress concentration.

Results. In the photoelastic analysis, the anterior abutments of the tripodal showed the highest stress, followed by the fully tripodal obturators, while, in FEA, the anterior abutments of the linear design received the most in both vertical and oblique load. The central incisor received the most stress in photoelastic (3 or more fringe orders) and FEA (687.3 and 150.1 MPa for vertical and oblique loads, respectively), followed by the lateral incisors. Upon posterior loading, the base of the defect of the linear design demonstrated the most stress in photoelastic (3 or more fringes) and FEA (94.3 and 130.5 MPa for vertical and oblique loads, respectively). The acrylic resin base obturator retained with Adams clasps demonstrated the lowest stress distribution in abutments and their supporting bone upon anterior and posterior loads.

Conclusions. Upon vertical and oblique load application, the fully tripodal design was comparable with the tripodal in terms of stress distribution. Both designs were better than the linear in response to the same loading. The stress was concentrated at the anterior palatal part of the obturator, the base of the defect, and the junction of the metal and acrylic resin part of the prostheses upon anterior and posterior loading, respectively. (J Prosthet Dent 2025;133:321.e1-e8)

Supported by the Ministry of Higher Education, Fundamental Research Grant Scheme (FRGS) (grant no. FRGS/1/2022/SKK0/USM/01/3)
The authors declare that they have no known competing financial interests or personal relationships that could have appeared to influence the work reported in this paper.

[a]Lecturer, Prosthetic Dental Sciences, College of Dentistry, Jouf University, Sakaka, Saudi Arabia; and Researcher, Prosthodontic Unit, School of Dental Sciences, Universiti Sains Malaysia, Kubang Kerian, Malaysia.
[b]Professor, Prosthodontics, Department of Preventive and Restorative Dentistry, College of Dental Medicine, University of Sharjah, Sharjah, United Arab Emirates; and Professor, Prosthodontic Unit, School of Dental Sciences, Universiti Sains Malaysia, Kubang Kerian, Malaysia.
[c]Professor, National Research Centre, Cairo, Egypt.
[d]Senior Lecturer, Prosthodontic Unit, School of Dental Sciences, Universiti Sains Malaysia, Kubang Kerian, Malaysia.
[e]Senior Lecturer, Craniofacial Imaging Laboratory, School of Dental Sciences, Universiti Sains Malaysia, Kubang Kerian, Malaysia; and Adjunct Professor, Dental Research Unit, Center for Transdisciplinary Research (CFTR), Saveetha Dental College, Saveetha Institute of Medical and Technical Sciences, Saveetha University, Chennai, India.

Clinical Implications

The fully tripodal design was comparable with the tripodal design regarding von Mises values and stress distribution on the supporting bone. Both designs were better than the linear design regarding the supporting bone but produced more stress on the abutments. The acrylic resin base obturator retained with Adams clasps still provides adequate options for managing palatal defects from a biomechanical point of view.

Patients who have received maxillectomy surgery can be provided with a removable obturator when surgical repair and implant-supported prostheses are not feasible.[1–3] The obturator is often used to restore various maxillary defects, facial deformities, deficient or absent lips, open occlusion, and lack of vertical dimensions.[3,4] In addition, obturators are an economically feasible and noninvasive treatment option.

Aramany classified 6 maxillary defects, of which the Aramany class I describes a defect involving the teeth and associated structures on one side extending to the midline without affecting the entire premaxilla.[5] Depending on support configuration, 2 designs are available to treat the Aramany class I maxillary defect: linear and tripodal.[6,7] In the linear design, support is provided by the premolars and molars of the dentate side, while in the tripodal design, the support is obtained from both anterior and posterior teeth.[6,7]

Photoelastic stress analysis uses photoelastic resin to assess stress distribution qualitatively and quantitatively. Although it has been used extensively in dentistry, its use in the maxillofacial discipline has been limited, possibly because of the complexity of the designs.[8,9] Studies have focused on implant-supported rather than conventional obturators, possibly because of the superimposition of the defect on the side to be evaluated.[10] To overcome the shortcomings of photoelastic stress analysis, finite element analysis (FEA) has been used in dentistry to simulate complicated structures that were difficult to replicate with the photoelastic approach. With rapid technological developments, FEA has become powerful in calculating stress distributions within complex dental models, especially where animal and human models cannot be deployed because of ethical concerns.[11–13]

Because of the nature of the defect, obturators are subjected to large stresses depending on the size and location of the defect, the remaining structures, and the weight of the prosthesis. These lead to more stress on the remaining tissues, causing bone resorption around the abutments, abutment loss, and prosthesis failure.[11] Decreasing the stress on the supporting structures and the obturators is essential for the adequate prognosis and longevity of the prostheses. In Aramany classes I and IV, the stress distribution in obturators with different framework base materials, including cobalt chromium and titanium alloys, has been evaluated using FEA. The study shows that von Mises stresses were higher for the cobalt chromium than the titanium base material, which demonstrated more deflection.[14,15] The stress distribution on the maxilla by the Aramany class IV obturator treated with surgical bone grafting has been evaluated using FEA.[16] The obturator tended to rotate around the resection line of the defect under a posterior load. The stress was concentrated on the alveolar ridge and the resection line[16] and was evaluated in a class IV obturator with 2 clasp designs, including multiple Roach and embrasure clasps. Compared with embrasure clasps, multiple Roach clasps led to reduced stress on the abutments.[17] In Aramany class I, the stress of single and 2-piece hollow bulb tripodal design obturators was evaluated under 3 loads, with no significant differences in stress distribution being reported between 1- and 2-piece obturators. The stress was concentrated closer to the palatal defect than other areas of the obturator.[18–20]

These studies suggest that Aramany class I obturators with different designs may have different biomechanics. However, the authors are unaware of evidence regarding stress evaluations of Aramany class I defects with different designs. Improving the current designs of Aramany class I prostheses for improved performance was also lacking,[11] making the choice among these designs more dependent on a conceptual than a scientific basis. The objective of the current study was to compare the stress distribution of these designs and an updated one. The null hypothesis was that no difference would be found in the stress distribution in the tested designs.

MATERIAL AND METHODS

This mathematical and in vitro study was conducted in the School of Dental Sciences, Universiti Sains Malaysia, with the Ethics and Research Committee, USM approval number JEPeM/21030222. The stress distribution of obturators with 4 designs, including conventional acrylic resin base, tripodal, linear, and fully tripodal designs, was evaluated using photoelastic stress analysis and FEA. The data were obtained as specified in part I of this study.[21] Computed tomography data of a 35-year-old patient who had received major head surgery were imported into a software program (Mimics 17.0; Materialise HQ) for segmentation to create an Aramany class I defect model. The produced model and teeth on the contralateral side were prepared with a 3D modeling software program (Meshmixer 5.3.4; Autodesk Inc) for printing using a 3D printer (Ender 3S1; Shenzhen Creality 3D Technology Co). For the printed model, 8 impressions were made using silicone duplicating materials (Replisil 22S; Silconic), while indexes were made to duplicate the printed teeth into 8 sets. To simulate the periodontal ligament space, the roots of the teeth were coated with 0.2-mm-thick polyvinyl siloxane (Flexceed Kit; GC Flexceed). To simulate the mucosa, a 2-mm-thick ethylvinylacetate sheet (Erkoflex: Erkodent Erich Kopp) was softened and adapted into the impressions. The produced acrylic teeth were then replaced and fixed into their corresponding location in the impression. The impression is then boxed and poured with an epoxy resin (Crystal clear epoxy; Craft E.) mixed in a ratio of 3:1 resin:hardener. After 24 hours, the teeth were separated using a thin metal disk, and the models were placed for 5 minutes under hot running water; then, the teeth were extracted from the models using maxillary forceps, and the rubber materials around the teeth and sockets were cleaned off. To simulate the periodontal ligament, a soft epoxy resin (Crystal clear soft epoxy; Craft E.) was rationed, mixed (3:1 resin to hardener), and poured into the sockets to fill the space occupied by the cleared rubber materials; the teeth were then relocated to their corresponding sockets. After 48 hours, the models were refined and prepared to receive the different obturators. There were 4 designs demonstrated by 8 models: 2 for acrylic resin base, 2 for linear, 2 for tripodal, and 2 for fully tripodal design obturators. As for the acrylic resin base obturator, 2 Adams clasps were placed on the maxillary first premolar and molar (Fig. 1A). Regarding the linear design, 2 mesial occlusal rest seats were prepared on both second premolar and molar teeth, and 2 distal occlusal rest seats were prepared on the first premolar and molar to receive the 4 occlusal rests of the 2 embrasure clasps (Fig. 1B). As for tripodal and fully tripodal designs, 2 cingulum rest seats were prepared on the central incisor and canine, 2 mesial occlusal rest seats were prepared on the first premolar and second molar, and 1 distal rest seat was prepared on the first molar. Although the preparation for tripodal and fully tripodal designs was identical, the framework designs differed. While the tripodal received a gingival approaching clasp on the central incisor and 2 retentive arms on the first and second molar, 3 clasps were added to the fully tripodal design, including a gingival approaching clasp on the central, reverse Akers on the first premolar, and embrasure clasp between the first and

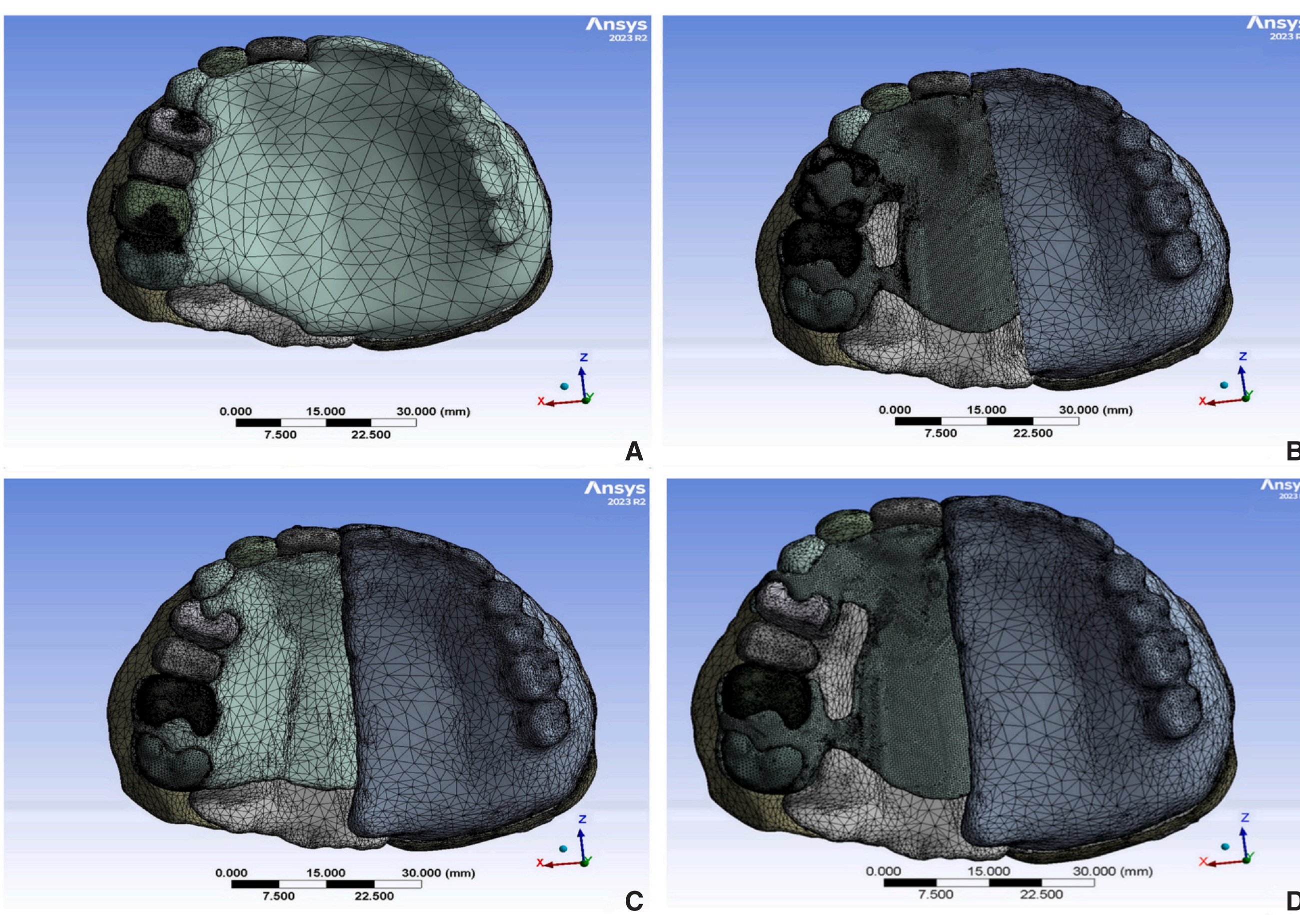

Figure 1. Mesh designs. A, Acrylic resin base obturator. B, Linear design obturator. C, Tripodal design obturator. D, Fully tripodal design obturator.

second molars to provide a tripodal support and retention configuration (Fig. 1C, D). After framework fabrication, the acrylic resin part was prepared using autopolymerizing acrylic resin (Self Curing; Holand Dental), and the fit of the obturators on their corresponding models was evaluated.

For the photoelastic stress analysis, the models were painted with paraffin oil and set in a circular polariscope setup. Because of the complexity of the models, 1 was used as a trial to identify the load that leads to the appearance of the fringes, and a load of 150 N was applied using a universal testing machine (Shimadzu; Shimadzu Corp). For each load application, a video recording was captured by a digital camera (Nikon DX; NIKON Corp) with a macrolens (AF-S NIKKOR 180–135 mm and 67 mm width) and exported to a computer. One recording was made anteriorly during the anterior load to evaluate the stress distribution on anterior teeth (central, lateral, and canine). For the posterior load, an additional video recording was made of the defect side to assess the stress distribution under the prostheses. No video record was applicable for the dentate side because of the overlap of the fringes in the defective part on those developed under the dentulous side. The fringe values were identified for each load under the prostheses and the abutments.

Descriptive statistics were used to quantitatively compare the stress among the different designs by counting the fringe orders around the roots of the abutments and on the defective side. The areas that showed more fringe orders indicated more stress concentration. Counting the fringe orders depended on the color transition from black to green as follows: black =0 fringe-order; the transition from red to blue =1 fringe-order; the transition from red to green =2 fringe-order; the transition from pink/green =3 fringe order.[22,23] The qualitative comparison was made through visual color mapping, while the areas with fringes closer to each other indicated more concentration and vice versa.[24]

Regarding the evaluation of stress distribution using FEA, after creating and meshing the models, as reported in part I of this study,[21] using static linear elastic FEA (using 4-node 3D tetrahedral full integration elements with a total number of nodes 2133577, 1935433, 1697520, and 1784732, and elements 1365410, 100905, 839327, and 954282 for acrylic resin base, linear, tripodal, and fully tripodal design obturators, respectively (Fig. 1), the base of the model was constrained, and 2 points, including the central incisor and molar area, were chosen to apply 2 loads, including vertical and oblique loads of 100 N. The vertical load was directed toward the tissue parallel to the long axis of the central incisor and perpendicular to the occlusal surface of the first molar, while the oblique load was directed toward the tissue with an angle of 30 degrees outward to a line parallel to the long axis of the same mentioned abutments (Fig. 2).

A workbench software program (ANSYS 2023R2; ANSYS Corp) was used to identify the influences of von Mises value within the prostheses and supporting structures. Descriptive statistics for von Mises values

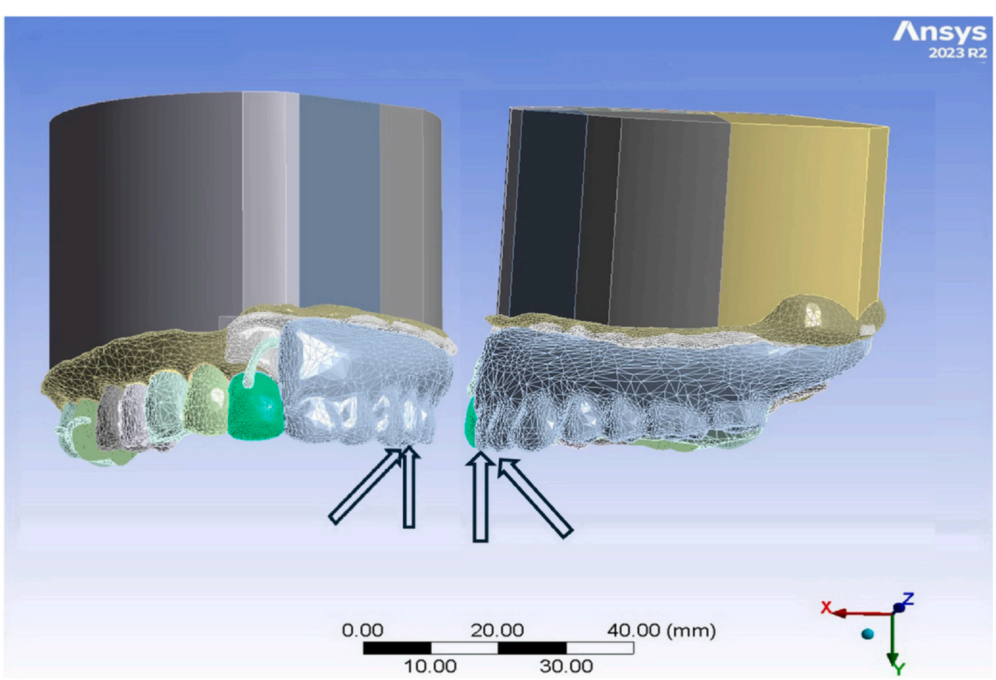

Figure 2. Direction of load on posterior and anterior denture teeth.

Table 1. Fringe orders in anterior teeth and their supporting structures of obturators with different designs under 150-N anterior loading

Supporting Structures	Different Designs			
	Acrylic Resin	Linear	Tripodal	Fully Tripodal
Central incisor	1	2	3	2
Lateral incisor	0	1	3	2
Canine	1	1	2	2
Supporting bone	1	3	3	2

have been reported to predict the failure of prosthetic components and supporting structures appropriately.[24] Higher von Mises values represent a higher risk of failure in prosthetic components or resorption in the supporting bone.[24–26] The outcomes enabled evaluation stress distribution using colored sketching.

RESULTS

The orders of the isochromatic fringes in the supporting bone under obturators of the different designs under anterior and posterior load are shown in Table 1. Regarding the central incisor, the acrylic resin obturators resulted in the lowest fringes, followed by the linear one (Fig. 3A, B), while the tripodal design produced more fringes, followed by the fully tripodal and linear designs. The fringes were concentrated at the apex and mesial side of the tooth next to the defect (Fig. 3C, D). Regarding the lateral incisor, the tripodal design produced the most fringes, followed by the fully tripodal design. The fringes were concentrated at the apex of the tooth and the interdental alveolar bone between it and the central incisor. Regarding the canine, the tripodal and fully tripodal designs showed more fringes than the acrylic resin base and linear designs. The fringes were concentrated at the apex of the tooth. Regarding the posterior loads, both linear and tripodal designs produced more fringes than the acrylic resin base and fully tripodal designs (Table 1, Fig. 4). The fringes were concentrated at the base of the defect in all obturators, extending to the anterior area in the linear one, where the fringes were closer.

Regarding the stress distribution upon 100 N anterior loads using FEA, as shown in Table 2, the linear design showed the highest von Mises values in both vertical and oblique loads (687.3 and 150.1 MPa for vertical and oblique loads, respectively), followed by the fully tripodal design in vertical load (418.1 MPa) and tripodal design in oblique load (129.2 MPa), in contrast with the acrylic resin base obturator, which demonstrated the lowest values (281.7 and 113.1 MPa for vertical and oblique load, respectively). The stress was concentrated in the supporting bone of the central incisor, followed by the lateral incisor, while the second molar tended to show the lowest von Mises values (Fig. 5A). Regarding the von Mises values in the different frameworks, the linear design showed the highest value (149.9 and 104.6 MPa in vertical and oblique load, respectively), in contrast with the fully tripodal and Adams clasps, which expressed the lowest value (Table 2). The stress was

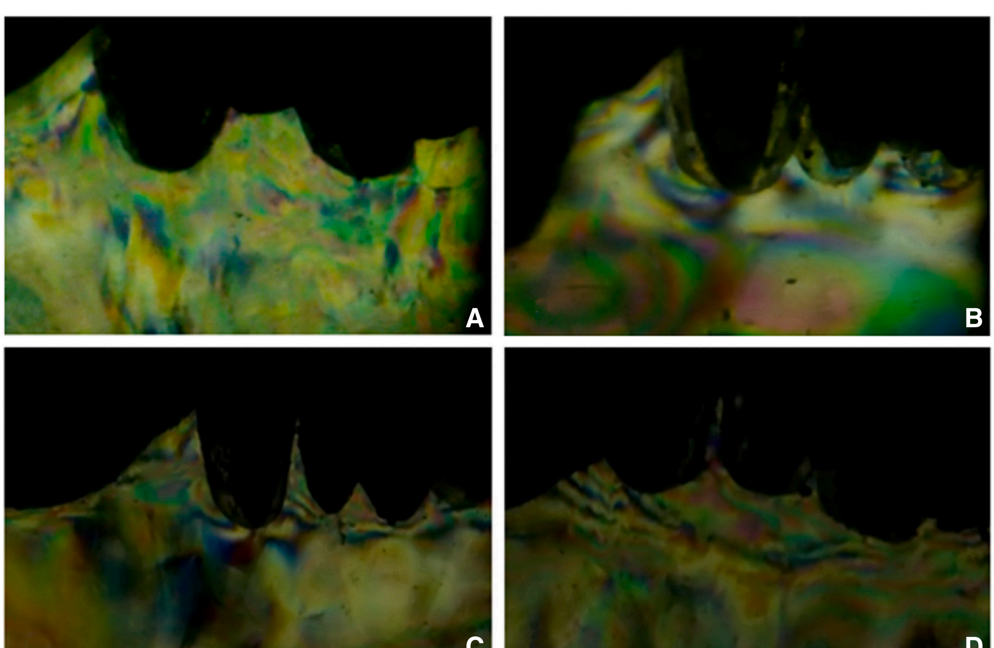

Figure 3. Fringe orders in anterior teeth of obturators with different designs under 150-N anterior loading. A, Acrylic resin base. B, Linear design. C, Tripodal design. D, Fully tripodal design.

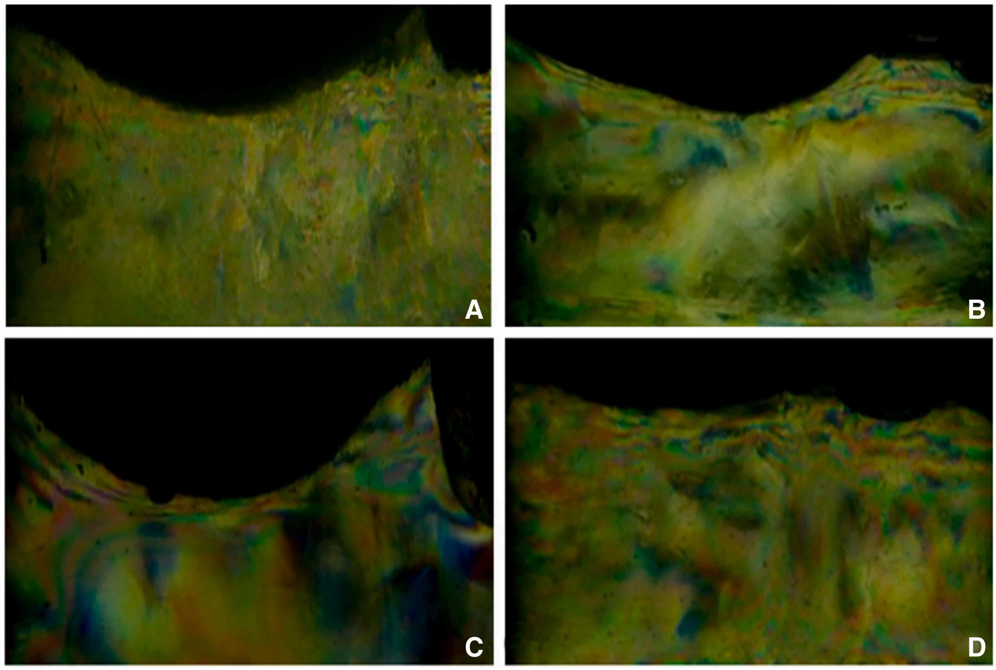

Figure 4. Fringe orders in supporting bone under obturators with different designs under 150-N anterior loading. A, Acrylic resin base. B, Linear design. C, Tripodal design. D, Fully tripodal design.

Table 2. von Mises stress values of assigned obturators under 100-N anterior vertical and oblique loads

Supporting Structures	Different Designs and Load Direction							
	Vertical Load (MPa)				Oblique Load (MPa)			
	Acrylic Resin	Linear	Tripodal	Fully Tripodal	Acrylic Resin	Linear	Tripodal	Fully Tripodal
Tooth	281.8	687.3	315.8	418.1	113.1	150.1	129.2	125.9
Periodontal ligament	0.2	0.3	0.1	0.6	0.5	0.3	0.2	0.5
Mucosa	0.1	0.2	0.1	0.1	0.1	0.1	0	0
Bone	6.6	59.7	20.8	20.2	12.6	49.7	24.6	20.9
Framework	119.5	149.9	87.8	65.6	41.4	104.6	60.4	49.1
Acrylic resin	33.4	145.4	55.6	126	7	46.7	32.6	23.9

concentrated in the anterior part of the major connector at the junction of the metal and acrylic portion of the prosthesis.

Table 3 shows the von Mises stress values with a 100-N posterior load. The fully tripodal design represented the highest von Mises values on the abutments (226.2 MPa),

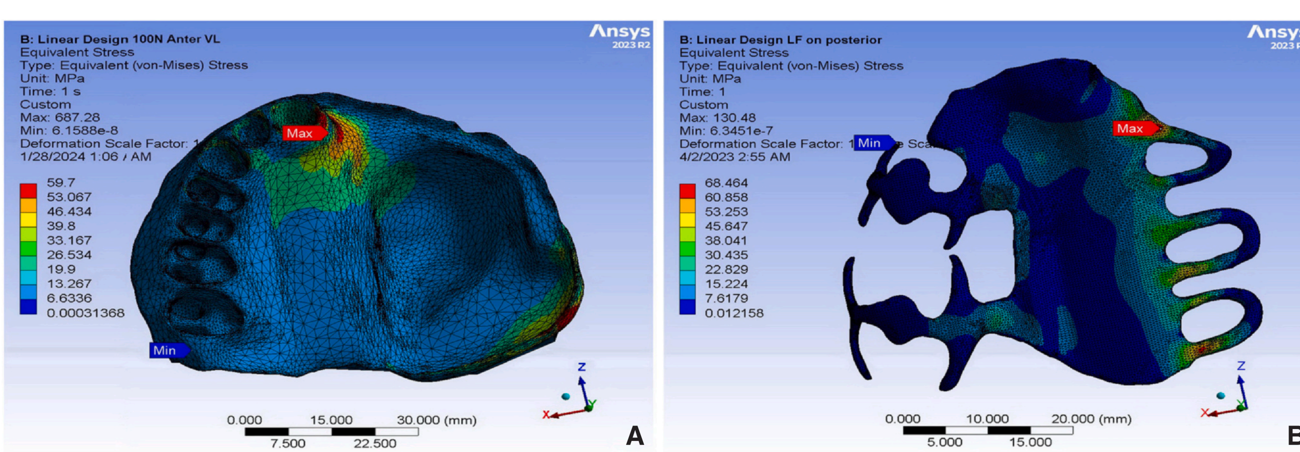

Figure 5. Stress distribution in supporting bone of linear design obturator under 100-N load. A, Anterior vertical load. B, Posterior oblique load.

Table 3. von Mises stress values of different obturators upon 100-N posterior vertical and oblique loads

Supporting Structures	Different Designs and Load Direction							
	Vertical Load (MPa)				Oblique Load (MPa)			
	Acrylic Resin	Linear	Tripodal	Fully Tripodal	Acrylic Resin	Linear	Tripodal	Fully Tripodal
Tooth	80.9	137.9	108	226.5	80.8	38.7	83.6	97.3
Periodontal ligaments	0.4	0.1	0.1	0.7	0.6	0.2	0.3	0.5
Mucosa	0.2	0.2	0.1	0.2	0.3	0.2	0.2	0.2
Bone	5.6	94.3	68.4	71.3	6.2	130.5	76.9	95.5
Framework	26	58.6	233.1	166.3	38.9	68.5	247	96.6
Acrylic resin	23.4	48.5	67.3	27.1	12.1	32.1	36.4	46

followed by the linear design during the vertical load (137.9 MPa) and tripodal design during the oblique load (83.6 MPa). The acrylic resin base obturator demonstrated the lowest value in the vertical load, while the linear design showed the lowest value in the oblique load. The stress was concentrated on the labial surface of the central incisor. The bone demonstrated the highest stress value in the linear design in both posterior loads. Regarding the prostheses, the tripodal design showed the highest values, followed by the fully tripodal design (Table 3). The acrylic resin base obturators demonstrated the lowest, followed by the linear design. The stress was concentrated at the junction between the metal and acrylic resin parts of the prosthesis (Fig. 5B).

DISCUSSION

The current study aimed to investigate and compare the stress distribution in the current and updated designs using photoelastic stress analysis and FEA. The study results showed differences in stress distribution among the different designs; therefore, the null hypothesis that no difference would be found in the stress distribution in the tested designs was rejected. Several studies have been conducted to evaluate the biomechanics of conventional obturator prostheses.[11] Some of these studies investigated the stress of obturators with various bulbs,[18,19] different clasps forms,[17] and different base materials.[14,15] The authors are unaware of a study that compared the universally used designs of the unilateral palatal defect.

FEA was used to overcome the limitations of photoelastic stress analysis, which include the overlapping of the fringes developed on the defect side on those produced around the abutments on the dentulous side. In the photoelastic stress analysis, a vertical load was applied individually to the anterior and posterior teeth of the obturator. In FEA, 2 loads, vertical and oblique, were applied on the same teeth. Adding oblique loads in FEA was done to simulate the lateral forces developed during mastication, which was not possible with photoelastic analysis.

Regarding the anterior loads, using the photoelastic analysis, the central incisor showed the highest stress compared with that of the lateral and canines, consistent with the FEA. These results were consistent with those of Wang et al,[20] who compared conventional obturators with those retained with zygomatic implants and reported a similar stress distribution in the conventional one. Using photoelastic analysis, the anterior abutments of the tripodal (followed by the fully tripodal) design showed the highest stress, while in FEA, those of the linear (followed by the fully tripodal) design showed the highest. The authors are unaware of previous studies that can be compared with the current study; however, the photoelastic analysis result can be explained as the tripodal and fully tripodal designs gaining support from anterior and posterior teeth, which caused the anterior teeth of both designs to receive more stress than those in linear and acrylic resin base obturators. From FEA and photoelastic analysis, the acrylic resin base obturator produced the least stress on the anterior abutments. The lower stress can be explained by the fact that the flexible acrylic resin base covers the entire palate and that the teeth on the contralateral side, extending occlusally to their maximum convexity, distribute the stress over additional areas, resulting in a decrease per unit area.

Regarding the posterior loads, although the anterior abutments received the highest stress in the fully tripodal, followed by the linear in the vertical load, and the tripodal design in the oblique load, the supporting bone of the defect showed the most stress in the linear design for both vertical and oblique loads. These findings can be explained by the fact that the tripodal and fully tripodal obturators received support from more teeth, which caused less movement of the obturator toward the tissue compared with the linear obturators.

The updated design was introduced to take advantage of linear and tripodal designs. The main advantages of the linear design were less tissue coverage and relief of the anterior teeth from the function of support and retention. However, relieving the anterior abutments from the support in the linear design resulted in a rotation of the prosthesis around the fulcrum axes passing through the premolar and molars. The main advantage of the tripodal design is the distribution of support over more abutments, giving a tripodal support configuration. However, adding only a clasp on the central incisor and molars resulted in more load on the central incisor during displacement. The fully tripodal obturator provided tripodal supportive (the same abutments in the tripodal design) and retentive (central, premolar, and molars) designs. In addition, it covered less tissue compared with the tripodal obturator.

Limitations of the photoelastic stress analysis and the FEA included that biological variations in the shape, number, and quality of the abutment and their periodontal support and the size and extent of the defect, patient attitude, oral hygiene, and posttreatment care were not simulated. These restrictions can be addressed by clinical studies to evaluate the clinical reliability of these designs.

CONCLUSIONS

Based on the findings of the current study, the following conclusions were drawn:

1. The fully tripodal and tripodal designs produced more stress on the abutments but less on the supporting bone in the defect base.
2. The stress of the linear design on the supporting bone was the highest compared with the fully tripodal and tripodal designs.
3. The acrylic resin base obturator retained with an Adams clasp provided an adequate stress distribution because of the design of the prosthesis.
4. The central incisor receives the highest stress from all obturator designs, followed by the lateral incisor.
5. The photoelastic stress analysis and FEA results were comparable regarding stress distribution evaluation.

REFERENCES

1. Wang LM, Tian YY, Liu XM, et al. Quality of life in patients with cancer-related Brown IIb maxillary defect: A comparison between conventional obturation rehabilitation and submental flap reconstruction. *Oral Oncol*. 2022;132:105980.
2. Chouksey G, Dugad J, Gupta V, Dholam K, Goel P, Choure R. Oral health-related quality of life after rehabilitation with maxillary obturators: A comparison of patients with maxillectomy defects associated with cancer and post-COVID-19 mucormycosis. *J Prosthet Dent* 2023.
3. Farook TH, Mousa MA, Jamayet NB. Method to control tongue position and open source image segmentation for cone-beam computed tomography of patients with large palatal defect to facilitate digital obturator design. *J Oral Maxillofac Surg Med Pathol*. 2020;32:61–64.
4. Mittal M, Sharma R, Kalra A, Sharma P. Form, function, and esthetics in prosthetically rehabilitated maxillary defects. *J Craniofac Surg*. 2018;29:e8–e12.
5. Aramany MA. Basic principles of obturator design for partially edentulous patients. Part I: Classification. *J Prosthet Dent*. 1978;40:554–557.
6. Aramany MA. Basic principles of obturator design for partially edentulous patients. Part II: design principles. *J Prosthet Dent*. 1978;40:656–662.
7. Parr GR, Tharp GE, Rahn AO. Prosthodontic principles in the framework design of maxillary obturator prostheses. *J Prosthet Dent*. 2005;93:405–411.
8. Pesqueira AA, Goiato MC, dos, Santos DM, Haddad MF, Andreotti AM, Moreno A. Stress analysis in oral obturator prostheses: Imaging photoelastic. *J Biomed Opt*. 2013;18:1–4.
9. Pesqueira AA, Goiato MC, da Silva EV, et al. Stress analysis in oral obturator prostheses, part II: Photoelastic imaging. *J Biomed Opt*. 2014;19:1–4.
10. Ramesh K, Hariprasad MP, Bhuvanewari S. Digital photoelastic analysis applied to implant dentistry. *Opt Lasers Eng*. 2016;87:204–213.
11. Mousa MA, Abdullah JY, Jamayet NB, Alam MK, Husein A. Biomechanical stress in obturator prostheses: A systematic review of finite element studies. *BioMed Res Int*. 2021;2021:1–12.
12. Mousa MA, Abdullah JY, Jamayet NB, et al. Biomechanics in removable partial dentures: A literature review of FEA-based studies. *BioMed Res Int*. 2021;2021:1–16.
13. Mousa MA, Jamayet N, Lynch E, Husein A. Biomechanical stress in removable complete dental prostheses: A narrative review of finite element studies. *J Int Oral Health*. 2020;12:413–419.
14. Arabbi KC, Shah TD, Sharanappa M, Subbaiah SK. A three-dimensional finite element analysis of Aramany class I obturator fabricated with different alloys. *J Pharm Bioallied Sci*. 2019;11:S24–S29.
15. Shah TD, Naveen YG, Kattimani P, Kamath G, Shah K, Raza A. Stress distribution deflection in an Aramany class II obturator fabricated with cobalt-chromium titanium alloys - 3D FEA. *Saudi Dent J*. 2019;31:251–257.
16. Miyashita ER, Mattos BS, Noritomi PY, Navarro H. Finite element analysis of maxillary bone stress caused by Aramany Class IV obturator prostheses. *J Prosthet Dent*. 2012;107:336–342.
17. Hase H, Shinya A, Yokoyama D, Shinya A, Takahashi Y. Three-dimensional finite element analysis of Aramany Class IV obturator prosthesis with different clasp designs. *Dent Mater J*. 2014;33:383–388.
18. Sudhan RH, Chander GN, Anitha KV. Finite element stress analysis of Aramany class I maxillectomy defect with single- and two-piece closed bulb obturators. *Gerodontology*. 2021;38:209–215.
19. Anitha KV, Gopi Chander N, Karthikeyan V, Hariharasudan R. Finite element analysis of displacement with single and two piece hollow bulb obturator prosthesis. *Med J Armed Forces India*. 2019;75:395–399.
20. Wang D, Qu A, Zhou H, Wang M. Biomechanical analysis of the application of zygoma implants for prosthesis in unilateral maxillary defect. *J Mech Med Biol*. 2016;16:1–16.
21. Mousa MA, Husein A, El-Anwar MI, Yusoff N, Abdullah J. Evaluation of the biomechanics of Aramany class I obturators with different designs using numerical and experimental methods. Part I: Retention and associated stress. *J Prosthet Dent* 2024.
22. Rodrigues RC, Faria AC, Macedo AP, de Mattos Mda G, Ribeiro RF. Retention and stress distribution in distal extension removable partial dentures with and without implant association. *J Prosthodont Res*. 2013;57:24–29.
23. Zaparolli D, Peixoto RF, Pupim D, Macedo AP, Toniollo MB, Mattos M. Photoelastic analysis of mandibular full-arch implant-supported fixed dentures made with different bar materials and manufacturing techniques. *Mater Sci Eng C Mater Biol Appl*. 2017;81:144–147.
24. Rungsiyakull C, Rungsiyakull P, Suttiat K, Duangrattanaprathip N. Stress distribution pattern in mini dental implant-assisted RPD with different clasp designs: 3D finite element analysis. *Int J Dent*. 2022;2022:2416888.
25. Eom JW, Lim YJ, Kim MJ, Kwon HB. Three-dimensional finite element analysis of implant-assisted removable partial dentures. *J Prosthet Dent*. 2017;117:735–742.
26. Shahmiri R, Das R. Finite element analysis of implant-assisted removable partial dentures: Framework design considerations. *J Prosthet Dent*. 2017;118:177–186.

Corresponding author:
Dr Johari Yap Abdullah
Craniofacial Imaging Laboratory
School of Dental Sciences
Universiti Sains Malaysia
Kubang Kerian, Kota Bharu, Kelantan 16150
MALAYSIA
Email: johariyap@usm.my

Acknowledgments
The authors thank Assoc Prof Yanti Johari (yjohari@usm.my), Dr NorWahida Yusoff (menorwahida@usm.my), Dr Nafij Jamayet (dr.nafij@gmail.com), Dr Ahmed Abbas (nawrozah@gmail.com) and the Prosthodontic Unit staff from the School of Dental Sciences at Universiti Sains Malaysia for their tremendous efforts in the accomplishment of this work.

CRediT authorship contribution statement
Mohammed A. Mousa: Conceptualization, Methodology, Software, and Writing, **Adam Husein**: Conceptualization, Methodology, Original draft preparation, **Mohammed I. El-Anwar**: Visualization, Methodology, and Software. **Azirrawani Ariffin**: Visualization, Methodology, **Johari Yap Abdullah**: Supervision, Validation, Reviewing, and Editing.

https://doi.org/10.1016/j.prosdent.2024.07.042